TMA4220 - PROJECT 1

OTTAR HELLAN, JOHANNES VOLL KOLSTØ AND GJERMUND LYCKANDER

1. Introduction

In this report we present a finite element method (FEM) formulation and implementation of the Poisson equation on the unit disk with both Dirichlet and Neumann boundary conditions. To this end, we first present the underlying theoretical formulation for our problem of choice and then present the methods we have used to implement the solver numerically. We then test our solver on simple test problems with varying number of elements and present our numerical findings.

The level of complexity involved in a two dimensional FEM-solver is markedly higher than for the single dimensional case, both the construction of the linear system and the construction of the discretized geometry are quite complicated. The focus of our report is on the theory behind, and solution of the final linear system $A_h \boldsymbol{u_h} = \boldsymbol{f}$, whilst the triangulation/construction of a discretized geometry was kindly provided along with the project description.

2. Theory

We implement a finite element solver for the Poisson problem on the unit disk either with pure homogeneous Dirichlet boundary conditions or with mixed homogeneous Dirichlet and Neumann boundary conditions.

2.1. Homogeneous Dirichlet.

In the case of pure homogeneous Dirichlet boundary conditions, the statement of the problem is

$$\begin{aligned} -\nabla^2 u &= f,\ (x,y) \in \Omega = \left\{(x,y) : x^2 + y^2 \leq 1\right\}, \\ u &= 0,\ (x,y) \in \partial\Omega. \end{aligned} \tag{2.1}$$

To solve the problem with the finite element method we need to transform the problem to a variational formulation. We do this by multiplying u with an element v of a Hilbert space X that u is a member of, and then integrating the product over the domain Ω. Starting from our Poisson Dirichlet problem we get

$$-\nabla^2 u = f \Rightarrow \iint_\Omega -\nabla^2 u\, v\, dx\, dy = \iint_\Omega f\, v\, dx\, dy,\ \forall\ v \in X.$$

With Green's formula, this is equivalent to

$$\iint_\Omega \nabla u \cdot \nabla v\, dx\, dy - \int_{\partial\Omega} \frac{\partial u}{\partial \boldsymbol{n}} v\, ds = \iint_\Omega f\, v\, dx\, dy,\ \forall v \in X$$

We then demand $v|_{\partial\Omega} = 0\, \forall v \in X$, the same as for u,

$$\begin{gathered} \iint_\Omega \nabla u \cdot \nabla v\, dx\, dy = \iint_\Omega f\, v\, dx\, dy,\ \forall v \in X \\ a(u,v) = l(v),\ \forall v \in X, \end{gathered}$$

where we introduce the bilinear form a and linear functional l in the last line. Our variational formulation is then finding the u satisfying the above,

$$\text{Find } u \in X \text{ such that } a(u,v) = l(v) \,\forall\, v \in X,$$

We need our Hilbert space X to be such that the operators a and l are well defined, and its elements fulfil any boundary conditions.

We want $a(u,v) < \infty$ for all $u, v \in X$, in particular when the two coincide. Then we have

$$|a(v,v)| = \left| \iint_\Omega \nabla v \cdot \nabla v \, dx\, dy \right| = \iint_\Omega (|v_x|^2 + |v_y|^2)\, dx\, dy < \infty \iff v_x, v_y \in L^2(\Omega),$$

so we need $v_x, v_y \in L^2(\Omega)$ for all $v \in X$. This is also sufficient when $u \neq v$, since with the Cauchy-Schwartz inequality

$$\begin{aligned} |a(u,v)| &= \left| \iint_\Omega u_x v_x + u_y v_y \, dx\, dy \right| \leq \left| \iint_\Omega u_x v_x \, dx\, dy \right| + \left| \iint_\Omega u_y v_y \, dx\, dy \right| \\ &\leq ||u_x||_{L^2(\Omega)} ||v_x||_{L^2(\Omega)} + ||u_y||_{L^2(\Omega)} ||v_y||_{L^2(\Omega)} < \infty, \end{aligned}$$

and we get that $a(u,v)$ is well defined for all $u, v \in X$.

We also need that $l(v) < \infty$ for all $v \in X$. We can bound l by

$$|l(v)| = \left| \iint_\Omega f\, v \, dx\, dy \right| \leq ||f||_{L^2(\Omega)} ||v||_{L^2(\Omega)} < \infty, \; \forall f, v \in L^2(\Omega),$$

again using the Cauchy-Schwartz inequality. Since in our case $f \in L^2(\Omega)$, it is enough to require that $v \in L^2(\Omega)$ for all $v \in X$ to have $l(v)$ well defined.

Combining the requirements that v, v_x and v_y are in $L^2(\Omega)$, we get that our space X must be a subspace of $H^1(\Omega)$. With the extra demand that $v|_{\partial\Omega} = 0$ fulfilling the boundary conditions, we get that

$$X = H_0^1(\Omega) = \left\{ v \in H^1(\Omega) : v|_{\partial\Omega} = 0 \right\} \tag{2.2}$$

is suitable.

Our variational formulation of (2.1) is then

$$\begin{aligned} &\text{Find } u \in H_0^1(\Omega) \text{ such that } a(u,v) = l(v) \,\forall\, v \in H_0^1(\Omega), \\ &a(u,v) = \iint_\Omega \nabla u \cdot \nabla v \, dx\, dy, \quad l(v) = \iint_\Omega f\, v \, dx\, dy. \end{aligned} \tag{2.3}$$

We can create a finite element formulation from (2.3) by finding an approximation to u through only considering elements of a finite-dimensional subspace of X. Instead of working with the infinite-dimensional space X, we search for a solution in $X_h \subset X$, and we define X_h by

$$X_h = \left\{ v \in X \,:\, v|_{T_k} \in \mathbb{P}_1(T_k), \, \forall\, T_k \in \mathcal{T} \right\}, \tag{2.4}$$

where the T_k are the elements in our triangulation $\mathcal{T}$. The basis functions $\{\varphi_i\}_{i=1}^n$ of X_h are linear polynomials that satisfy

$$X_h = \text{span}\{\varphi_i\}_{i=1}^n, \quad \varphi_j(\boldsymbol{x}_i) = \delta_{ij},$$

where the $\boldsymbol{x}_i$ are the nodes in our triangulation.

This reduced problem is expressed as

$$\text{Find } u_h \in X_h \text{ such that } a(u_h, v_h) = l(v_h), \; \forall\, v_h \in X_h. \tag{2.5}$$

We can write u_h as $u_h = \sum_{i=1}^{n} u_h^i \varphi_i(x,y)$. We define the matrix $A \in \mathbb{R}^{n\times n}$ and the vectors $\boldsymbol{u}, \boldsymbol{f} \in \mathbb{R}^n$ by

$$\begin{aligned} A &= [A_{ij}] = [a(\varphi_i, \varphi_j)] \\ \boldsymbol{u} &= [u_h^i] \\ \boldsymbol{f} &= [f^i] = [l(\varphi_i)] \end{aligned}$$

and represent each function $v_h = \sum_{i=1}^{n} v_h^i \varphi(x,y) \in X_h$ by the vector

$$\boldsymbol{v} = [v_h^i].$$

The left side of the expression in (2.5) is

$$\begin{aligned} a(u_h, v_h) &= a\left(\sum_{i=1}^{n} u_h^i \varphi_i, \sum_{j=1}^{n} v_h^j \varphi_j\right) = \sum_{i=1}^{n} u_h^i a(\varphi_i, \sum_{j=1}^{n} v_h^j \varphi_j) \\ &= \sum_{i=1}^{n}\sum_{j=1}^{n} u_h^i v_h^j a(\varphi_i, \varphi_j) = \sum_{i=1}^{n}\sum_{j=1}^{n} u_h^i v_h^j A_{ij} \\ &= \boldsymbol{v}^T A \boldsymbol{u} \end{aligned}$$

and the right side of the expression in (2.5) is

$$\begin{aligned} l(v_h) &= l\left(\sum_{i=1} u_h^i \varphi_i\right) = \sum_{i=1} u_h^i l(\varphi_i) = \sum_{i=1} u_h^i f^i \\ &= \boldsymbol{v}^T \boldsymbol{f}. \end{aligned}$$

Therefore, (2.5) is equivalent to

$$\text{Find } u_h \in X_h \text{ s.t. } \boldsymbol{v}^T A \boldsymbol{u} = \boldsymbol{v}^T \boldsymbol{f},\ \forall v_h \in X_h.$$

Since $\boldsymbol{v}^T A \boldsymbol{u} = \boldsymbol{v}^T \boldsymbol{f}$ for all $\boldsymbol{v} \in \mathbb{R}^n$, an equivalent problem to (2.5) is

$$\begin{aligned} &\text{Find } \boldsymbol{u} \in \mathbb{R}^n \text{ s.t. } A\boldsymbol{u} = \boldsymbol{f}, \\ &A_{ij} = a(\varphi_i, \varphi_j),\ f^i = l(\varphi_i), \end{aligned} \tag{2.6}$$

which is what our solver computes.

Because of the way the basis functions of X_h are defined, they all have local support, the support is for each basis function limited to a handful of elements. Therefore the stiffness matrix A is very sparse, making computations much more efficient. Indeed, A is symmetric and

$$\boldsymbol{v}^{\mathrm{T}} A \boldsymbol{v} = a(v_h, v_h) = \iint_{\Omega} ||\nabla v_h||^2_{L^2(\Omega)}\, dx\, dy > 0,\ \forall\, v_h \neq 0 \in X_h,$$

so A is also positive-definite. Therefore, A is symmetric, positive-definite, and many powerful numerical methods such as the conjugate gradient method can be applied.

The matrix A as defined here is singular, since we have not yet dealt with the boundary conditions, and therefore the system will not be solvable for $\boldsymbol{u}$ just yet. We deal with the boundary conditions in section 2.3, after first detailing the finite element formulation for the case of mixed Neumann-homogeneous Dirichlet boundary conditions.

2.2. **Neumann-Homogeneous Dirichlet.** With mixed Neumann-homogeneous Dirichlet boundary conditions, the Poisson equation we solve is stated as

$$\begin{aligned} -\nabla^2 u &= f,\ (x,y) \in \Omega = \big\{(x,y) : x^2 + y^2 \leq 1\big\} \\ u &= 0,\ (x,y) \in \partial\Omega_D = \big\{(x,y) : x^2 + y^2 = 1,\ y < 0\big\} \\ \frac{\partial u}{\partial \boldsymbol{n}} &= g,\ (x,y) \in \partial\Omega_N = \big\{(x,y) : x^2 + y^2 = 1,\ y > 0\big\} \end{aligned} \tag{2.7}$$

Creating our variational formulation, we start as before, with $-\nabla^2 u = f$ and proceed with

$$-\nabla^2 u = f \Rightarrow \iint_\Omega -\nabla^2 u\, v\, dx\, dy = \iint_\Omega f\, v\, dx\, dy,\ \forall\, v \in X.$$

With the use of Green's formula, we get

$$\iint_\Omega \nabla u \cdot \nabla v\, dx\, dy - \int_{\partial\Omega} \frac{\partial u}{\partial \boldsymbol{n}} v\, ds = \iint_\Omega f\, v\, dx\, dy,\ \forall v \in X$$

$$\iint_\Omega \nabla u \cdot \nabla v\, dx\, dy - \int_{\partial\Omega_D} \frac{\partial u}{\partial \boldsymbol{n}} v\, ds - \int_{\partial\Omega_N} \frac{\partial u}{\partial \boldsymbol{n}} v\, ds = \iint_\Omega f\, v\, dx\, dy,\ \forall v \in X$$

Also here we demand that $v|_{\partial\Omega_D} = 0,\ \forall\, v \in X$, as is the case for u, and impose the Neumann boundary condition $\partial u/\partial \boldsymbol{n}|_{\partial\Omega_N} = g$, giving

$$\iint_\Omega \nabla u \cdot \nabla v\, dx\, dy - \int_{\partial\Omega_N} g\, v\, ds = \iint_\Omega f\, v\, dx\, dy,\ \forall v \in X$$

$$\iint_\Omega \nabla u \cdot \nabla v\, dx\, dy = \iint_\Omega f\, v\, dx\, dy + \int_{\partial\Omega_N} g\, v\, ds,\ \forall v \in X$$

$$a(u,v) = l(v),\ \forall v \in X.$$

As before, the bilinear form a is defined as

$$a(u,v) = \iint_\Omega \nabla u \cdot \nabla v\, dx\, dy,$$

but now the linear functional l incorporates the Neumann condition and is defined as

$$l(v) = \iint_\Omega f\, v\, dx\, dy + \int_{\partial\Omega_N} g\, v\, ds.$$

By theorem (2.3) of Quarteroni[1], there exists a unique linear, continuous restriction

$$\gamma_{\partial\Omega_N} : H^1(\Omega) \to L^2(\partial\Omega_N),$$

such that

$$\gamma_{\partial\Omega_N} v = v|_{\partial\Omega_N}\, \forall\, v \in H^1(\Omega) \cap C^0(\overline{\Omega}).$$

Since $\gamma_{\partial\Omega_N}$ is linear and continuous, there exists a $C_\gamma > 0$ such that

$$||\gamma_{\partial\Omega_N} v||_{L^2(\partial\Omega_N)} \leq C_\gamma ||v||_{H^1(\Omega)},\ \forall\, v \in H^1(\Omega).$$

We implicitly assume that the integral over the boundary in the linear functional l is performed with the restriction $\gamma_{\partial\Omega_N}$ and then

$$\begin{aligned} \left| \int_{\partial\Omega_N} g\, v\, ds \right| &\leq ||g||_{L^2(\partial\Omega_N)}\, ||\gamma_{\partial\Omega_N} v||_{L^2(\partial\Omega_N)} \\ &\leq C_\gamma ||g||_{L^2(\partial\Omega_N)}\, ||v||_{H^1(\Omega)} < \infty \\ \Rightarrow |l(v)| &< \infty, \end{aligned}$$

so the functional $l(v)$ is well defined when $g \in L^2(\Omega)$, which in this case holds. Therefore no further restrictions on X need to be made, and we define our space as

$$X = H^1_D = \left\{ v \in H^1 \,:\, v|_{\partial\Omega_D} = 0 \right\}.$$

We can now state our variational formulation for the mixed Neumann-homogeneous Dirichlet problem as

$$\text{Find } u \in H^1_D(\Omega) \text{ such that } a(u,v) = l(v) \,\forall\, v \in H^1_D(\Omega), \tag{2.8}$$

$$a(u,v) = \iint_\Omega \nabla u \cdot \nabla v \, dx\, dy, \quad l(v) = \iint_\Omega f\, v \, dx\, dy + \int_{\partial\Omega_N} g\, v \, ds.$$

This formulation can be transformed into a linear system in much the same way as for the pure homogeneous Dirichlet problem, the change will be in how the $\boldsymbol{f}$-vector is calculated.

2.3. **Boundary conditions in the linear system.** The linear systems (2.6) and the one obtained from the mixed boundary conditions case are singular as presented, because the boundary conditions have not yet been applied. We apply the boundary conditions to the edge nodes, the ones lying on $\partial\Omega$.

For nodes on the part of the boundary $\partial\Omega_N$ where the Neumann conditions are enforced, the boundary conditions in the linear system are already included in the construction of the linear system, since the boundary conditions are expressed as a part of the functional l defining the right hand side vector $\boldsymbol{f}$.

In the case that a node has a homogeneous Dirichlet boundary condition, the portion of the system corresponding to the node is redundant and we remove it from the system. Since

$$v|_{\partial\Omega_D} = 0, \,\forall\, v \in X_h,$$

necessarily it follows that $\varphi_i \notin X_h$ for any i where $\boldsymbol{x}_i \in \partial\Omega_D$. Since row i of A describes the interactions of the other basis functions and φ_i and φ_i is not part of X_h, we remove row i from the stiffness matrix A. Seeing as $u^i = u(\boldsymbol{x}_i) = 0$, we also know that column i of A gives no effect on the system, so we also remove column i from the stiffness matrix A.

After these modifications are done for all boundary nodes, the stiffness matrix A is non-singular and the unique solution of (2.6) gives the finite element approximation to the solution of the Poisson equation.

2.4. **Convergence.** By theorem (4.7) of Quarteroni[1] we have that for u_h given by finite element methods of degree one and $u \in H^2(\Omega)$, the error estimate

$$||u - u_h||_{L^2(\Omega)} \leq Ch^2 |u|_{H^2(\Omega)}$$

holds, with C a constant independent of u and h. Since the u we consider in our tests, given in (4.2), is smooth on Ω, we see that $|u|_{H^2(\Omega)} < \infty$ and

$$||u - u_h||_{L^2(\Omega)} \leq Ch^2,$$

with C a new constant independent of u and h. Therefore we expect to find quadratic convergence as a function of triangulation diameter in our experiments.

3. Implementation

Gaussian Quadrature. In order to construct the matrix A and the source vector $\boldsymbol{f}$ used in the Galerkin projection method, one needs to evaluate up to several integrals per element covering the solution domain Ω. Finding analytical expressions for these integrals over general domains and arbitrary source functions is in general intractable, and one therefore makes use of numerical integration techniques, or quadratures, to evaluate many of these integrals. The quadrature method of choice for this report is Gaussian quadrature, owing to its high precision for few evaluations of the integrand.

In Gaussian quadrature on a line, all integrals are assumed to be on the segment $[-1, 1] \subset \mathbb{R}$. In order to facilitate more general integrals between points a and b in either $\mathbb{R}^1$ or $\mathbb{R}^2$, one may parametrize the line $\overline{ab}$ by $\eta \in [-1, 1]$, with $x(\eta) = \frac{1}{2}((b-a)\eta + (b+a))$. The quadrature formula for integrating a function f over the line $\overline{ab}$ then becomes

$$\int_a^b f \, dl \approx \frac{||b-a||_2}{2} \sum_{q=1}^{N_q} \rho_q \cdot f(x(\eta_q)), \tag{3.1}$$

where weights and abscissas, ρ_q and η_q respectively, are specified in table 1a.

In order to perform Gaussian quadrature on triangles in $\mathbb{R}^2$, we use the weights and abscissas specified in table 1b from [2], where area coordinates are used. If (p_1, p_2, p_3) are the three vertices of a triangle K, the mapping $x(\boldsymbol{\eta}) = \sum_{i=1}^{3} \eta_i p_i$ returns the global coordinates in the triangle K from the area coordinates. The Gaussian quadrature formula for integrating over K then becomes

$$\iint_K f \, dA \approx \iint_K dA \cdot \sum_{q=1}^{N_q} \rho_q f(x(\boldsymbol{\eta_q})). \tag{3.2}$$

Transformation to Reference triangle. For ease of computation, it is beneficial to transform the integral over each element T_k into an integral over the reference triangle $T_{\text{ref}} = \{(r, s) \in \mathbb{R}^2 : r \in [0, 1], s \in [0, 1 - r]\}$. Any triangular element is characterised by its three vertices, $(p_1, p_2, p_3)_{T_k} \in \mathbb{R}^{2\times 3}$, and from them we can build a transformation F_{T_k} from the reference element to T_k:

$$\begin{pmatrix} x \\ y \end{pmatrix} = F_{T_k} \begin{pmatrix} r \\ s \end{pmatrix} = \begin{bmatrix} p_2 - p_1 | p_3 - p_1 \end{bmatrix} \begin{pmatrix} r \\ s \end{pmatrix} + p_1 = J_{T_k} \begin{pmatrix} r \\ s \end{pmatrix} + p_1, \tag{3.3}$$

with J_{T_k} being the Jacobian of the transformation. Similarly, we have the inverse transformation $F_{T_k}^{-1}$

$$\begin{pmatrix} r \\ s \end{pmatrix} = F_{T_k}^{-1} \begin{pmatrix} x \\ y \end{pmatrix} = J_{T_k}^{-1} \left(\begin{pmatrix} x \\ y \end{pmatrix} - p_1 \right). \tag{3.4}$$

N_q	η_q	ρ_q
1-point rule	0	2
2-point rule	$-\sqrt{1/3}$	-1
	$\sqrt{1/3}$	1
3-point rule	$-\sqrt{3/5}$	5/9
	0	8/9
	$\sqrt{3/5}$	5/9
4-point rule	$-\sqrt{\frac{3+2\sqrt{6/5}}{7}}$	$\frac{18-\sqrt{30}}{36}$
	$-\sqrt{\frac{3-2\sqrt{6/5}}{7}}$	$\frac{18+\sqrt{30}}{36}$
	$\sqrt{\frac{3-2\sqrt{6/5}}{7}}$	$\frac{18+\sqrt{30}}{36}$
	$\sqrt{\frac{3+2\sqrt{6/5}}{7}}$	$\frac{18-\sqrt{30}}{36}$

(A) 1D Gauss quadrature points and weights.

N_q	$\boldsymbol{\eta_q} = (\eta_1, \eta_2, \eta_3)$	ρ_q
1-point rule	(1/3, 1/3, 1/3)	1
3-point rule	(1/2, 1/2, 0)	1/3
	(1/2, 0, 1/2)	1/3
	(0, 1/2, 1/2)	1/3
4-point rule	(1/3, 1/3, 1/3)	-9/16
	(3/5, 1/5, 1/5)	25/48
	(1/5, 3/5, 1/5)	25/48
	(1/5, 1/5, 3/5)	25/48

(B) 2D Gauss quadrature points (in area coordinates) and weights.

TABLE 1. Gauss quadrature points and weights for 1D and 2D.

When one then evaluates the contribution to A_{ij} from an element T_k, the integral transforms as

$$\begin{aligned}\iint_{T_k} \nabla\phi_i(x,y)\cdot\nabla\phi_j(x,y)\,dx\,dy &= \iint_{T_{\text{ref}}} J_{T_k}^{-\mathrm{T}}\nabla\hat{\phi}_i(r,s)\cdot J_{T_k}^{-\mathrm{T}}\nabla\hat{\phi}_j(r,s)|J_{T_k}|\,dr\,ds,\\ &= J_{T_k}^{-\mathrm{T}}\nabla\hat{\phi}_i\cdot J_{T_k}^{-\mathrm{T}}\nabla\hat{\phi}_j|J_{T_k}|\iint_{T_{\text{ref}}} dr\,ds,\\ &= \frac{|J_{T_k}|}{2}J_{T_k}^{-\mathrm{T}}\nabla\hat{\phi}_i\cdot J_{T_k}^{-\mathrm{T}}\nabla\hat{\phi}_j.\end{aligned}$$

where $J_{T_k}^{-\mathrm{T}}$ denotes the transpose of the inverse Jacobian for element T_k, and $\hat{\phi}_i(r,s)$ denotes the basis functions in the reference element. As all basis functions are linear, and the Jacobians are constant, we can pull them out of the integral and arrive at a closed-form expression.

Contributions to the source vector f^i are transformed to integrals over the reference element in the same manner, but the integrand is not constant in that case. To evaluate the integrals we then use 4-point Gaussian quadrature over the reference element.

4. Results

We test our solver against problems with known solutions. For the case of only homogeneous Dirichlet boundary conditions, the problem is stated as

$$\begin{aligned}-\nabla^2 u &= f,\ (x,y)\in\Omega = \left\{(x,y) : x^2+y^2\le 1\right\}\\ u &= 0,\ (x,y)\in\partial\Omega\\ f &= -8\pi\cos(2\pi r^2) + 16\pi^2 r^2\sin(2\pi r^2),\end{aligned} \tag{4.1}$$

with the solution

$$u(x,y) = \sin(2\pi(x^2+y^2)). \tag{4.2}$$

In polar coordinates, the form of the Laplace operator is

$$\nabla^2 = \frac{\partial^2}{\partial r^2} + \frac{1}{r}\frac{\partial}{\partial r} + \frac{1}{r^2}\frac{\partial^2}{\partial \theta^2}$$

and thus

$$\begin{aligned}
\nabla^2 u &= \frac{\partial^2 u}{\partial r^2} + \frac{1}{r}\frac{\partial u}{\partial r} + \frac{1}{r^2}\frac{\partial^2 u}{\partial \theta^2} \\
&= \frac{\partial}{\partial r}\left(4\pi r\cos(2\pi r^2)\right) + \frac{1}{r}\left(4\pi r\cos(2\pi r^2)\right) \\
&= 4\pi\cos(2\pi r) - 16\pi^2 r^2\sin(2\pi r^2) + 4\pi\cos(2\pi r^2) \\
&= 8\pi\cos(2\pi r^2) - 16\pi^2 r^2\sin(2\pi r^2) \\
&= -f.
\end{aligned}$$

Also, $u(x,y) = \sin(2\pi\cdot 1) = 0$, $\forall\,(x,y) \in \partial\Omega$, so (4.2) is a solution to (4.1).

For the mixed Neumann-homogeneous Dirichlet boundary conditions case, we state our test problem as

$$\begin{aligned}
-\nabla^2 u &= f,\ (x,y) \in \Omega = \left\{(x,y) : x^2+y^2 \le 1\right\} \\
u &= 0,\ (x,y) \in \partial\Omega_D = \left\{(x,y) : x^2+y^2 = 1,\ y < 0\right\} \\
\frac{\partial u}{\partial \boldsymbol{n}} &= g,\ (x,y) \in \partial\Omega_N = \left\{(x,y) : x^2+y^2 = 1,\ y > 0\right\} \\
f &= -8\pi\cos(2\pi r^2) + 16\pi^2 r^2\sin(2\pi r^2) \\
g &= 4\pi r\cos(2\pi r^2)
\end{aligned} \tag{4.3}$$

To verify that (4.2) is a solution to (4.3) it suffices to show that the Neumann condition holds on $\partial\Omega_N$. Since the normal vector on $\partial\Omega$ is the radial vector, we see that

$$\frac{\partial u}{\partial \boldsymbol{n}}|_{\partial\Omega_N} = \frac{\partial u}{\partial r}|_{\partial\Omega_N} = \frac{\partial}{\partial r}\sin(2\pi r^2) = 4\pi r\cos(2\pi r^2) = g$$

and the Neumann boundary condition is fulfilled. Therefore (4.2) is a solution to (4.3).

We test our methods on the Dirichlet boundary condition (4.1) and mixed boundary condition (4.3) test problems and measure the relative errors of the approximate solutions in the $L^2(\Omega)$-norm.

To calculate the $L^2(\Omega)$-norm of the errors $u - u_h$, we use Gaussian quadrature with four quadrature points on each element, giving us

$$||u-u_h||^2_{L^2(\Omega)} = \iint_\Omega (u-u_h)^2\,dx\,dy = \sum_{T_k\in\mathcal{T}} \iint_{T_k} (u-u_h)^2\,dx\,dy$$

$$\iint_{T_k} (u-u_h)^2\,dx\,dy \approx \sum_{i=1}^{4} \rho_i^k \left(u(q_i^k) - u_h(q_i^k)\right)^2$$

$$||u-u_h||^2_{L^2(\Omega)} \approx \sum_{T_k\in\mathcal{T}} \sum_{i=1}^{4} \rho_i^k \left(u(q_i^k) - u_h(q_i^k)\right)^2,$$

where ρ_i^k and q_i^k are the quadrature weights and points obtained by transforming from the reference triangle to the element.

We measure the convergence rate of our method on the test problems by attempting to fit our observations to the linear regression model

$$\log(E) = \alpha + \beta \log(h) \iff E = \alpha h^\beta,$$

where E is the relative error of u_h measured in the $L^2(\Omega)$-norm and h is the diameter of our triangulation, that is, the greatest distance between two nodes of an element found in the triangulation. The relative errors in our two test problems as a function of h, along with measured convergence rates, are found in figure 1.

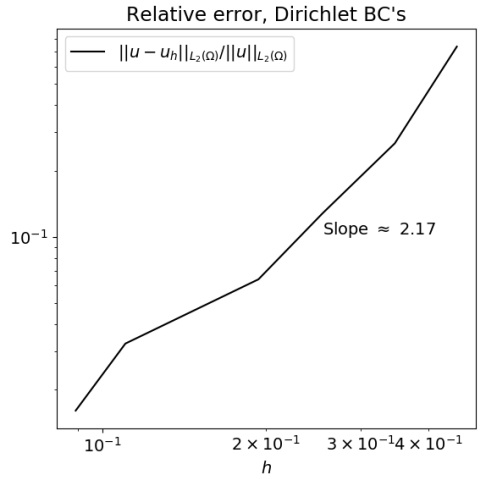

(A) The relative error of our FEM solution to (4.1) as a function of the triangulation diameter h. The approximate slope of 2.17 in log-log coordinates indicates an approximate convergence rate of $||u - u_h||_{L^2(\Omega)} \approx Ch^{2.17}$.

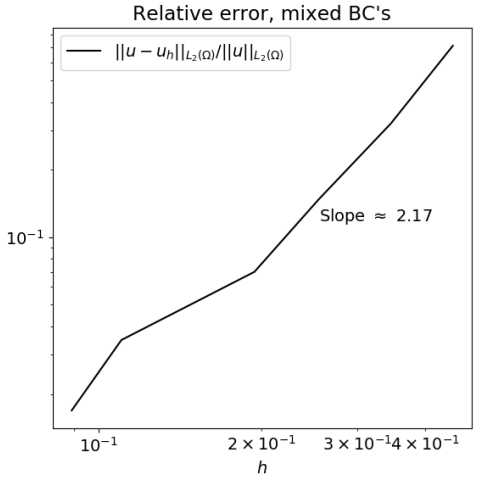

(B) The relative error of our FEM solution to (4.3) as a function of the triangulation diameter h. The approximate slope of 2.17 in log-log coordinates indicates an approximate convergence rate of $||u - u_h||_{L^2(\Omega)} \approx Ch^{2.17}$.

FIGURE 1. Convergence rates on the homogeneous Dirichlet and mixed boundary conditions. The measured convergence rates are not identical, but coincide due to round off-errors.

For the Dirichlet test problem, (4.1), we obtained a convergence approximately proportional to $h^{2.17}$, as can be seen in figure 1a. For the mixed boundary problem, (4.3), a convergence approximately proportional to $h^{2.17}$ was obtained.

Our solution to the mixed boundary conditions test problem (4.3) can be seen in figure 2. Our solutions to (4.1) and (4.3) are similar on the interior, as can be seen in figures 3a and 3b. It can also be seen that the two solutions have similar errors on the part of the boundary with $y < 0$, where both systems have equal Dirichlet boundary conditions. The error on the Neumann boundary of (4.3) is larger than that on the Dirichlet boundary of (4.1) for $y > 0$.

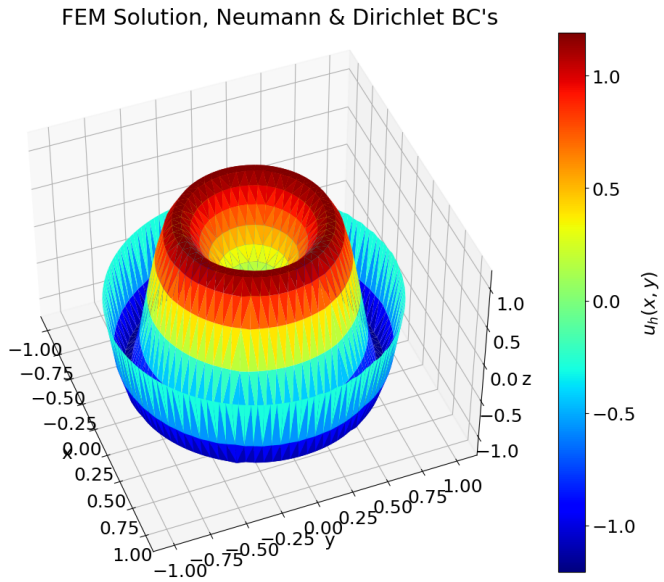

FIGURE 2. Plot showing the numerical solution to (4.3)

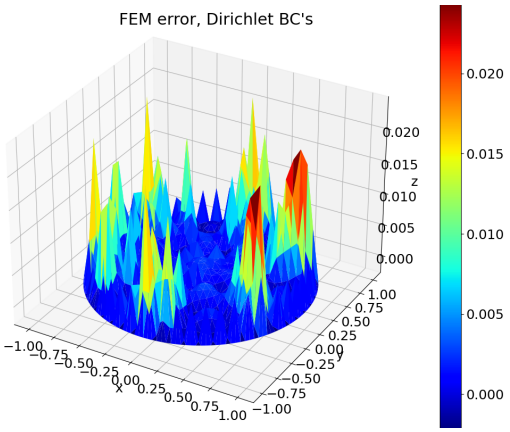

(A) Plot showing the absolute value of the error of the solution to (4.1) with $N = 1000$ nodes.

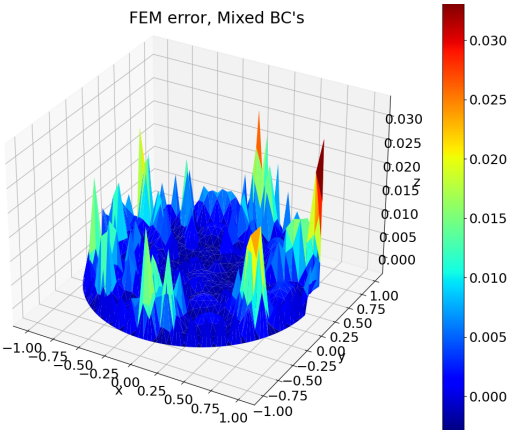

(B) Plot showing the absolute value of the error of the solution to (4.3) with $N = 1000$ nodes.

FIGURE 3. Absolute Error $|u - u_h|$ for Dirichlet and mixed boundary conditions respectively.

5. Discussion

Through the process of building and testing this solver, there are several key takeaways. Although there is considerable work in rewriting a differential equation on strong form into its weak formulation as a variational problem, this methodology holds several advantages over other methods of solving partial differential equations, for example Finite Difference methods.

Perhaps most easily observed, is the ease with which the Finite Element method can be adapted to different underlying geometries. As long as the triangulation is of sufficient quality, one can extend the solution domain to approximate curved domains, without needing to find several different differentiation rules for use in different parts of the domain with differing lengths between points, as might be necessary in order to keep the order of convergence one wants to attain in the Finite Difference approach.

The obtained convergence rate of $||u - u_h||_{L^2(\Omega)} \approx Ch^{2.17}$ is larger than the convergence rate proportional to h^2 we expect from the theory, as shown in subsection 2.4. This is surprising, but not altogether too implausible, seeing as the test problem we study is quite well behaved, for example it is infinitely differentiable on the entirety $\mathbb{R}^2$.

6. Conclusion

Our finite element implementation solves the Poisson problem on the unit disk with Dirichlet boundary conditions and with mixed Dirichlet and Neumann boundary conditions. The error is greatest at the boundary for both solutions, and both solutions obtain a convergence approximately proportional to $h^{2.17}$, which is slightly better than the h^2 convergence rate expected from the theory.

With this solver it should be possible to find approximations to Poisson's equation on domains where one does not have a tractable analytical solution, and for future investigations this would be interesting to investigate.

References

[1] Alfio Quarteroni and Silvia Quarteroni. *Numerical models for differential problems*. Vol. 2. Springer, 2009.

[2] GR Cowper. "Gaussian quadrature formulas for triangles". In: *International Journal for Numerical Methods in Engineering* 7.3 (1973), pp. 405–408.